Electronic Supplementary Material (ESI) for Nanoscale.

Supporting Information

In situ monitoring the electrochemically induced phase transition of thermodynamic metastable 1T-MoS_2 at nanoscale†

Junxiao Huang [a], Xuelei Pan [a], Xiaobin Liao [a], Mengyu Yan [b], Bruce Dunn [c], Wen Luo*[ad], Liqiang Mai*[a]

a. State Key Laboratory of Advanced Technology for Materials Synthesis and Processing, Wuhan University of Technology, Wuhan 430070, China

b. Materials Science and Engineering Department, University of Washington, Seattle, Washington 98195-2120, United States

c. Materials Science and Engineering, University of California, Los Angeles, California 90096, United States

d. Department of Physics, School of Science, Wuhan University of Technology, Wuhan 430070, China

Email: luowen_1991@whut.edu.cn ; mlq518@whut.edu.cn

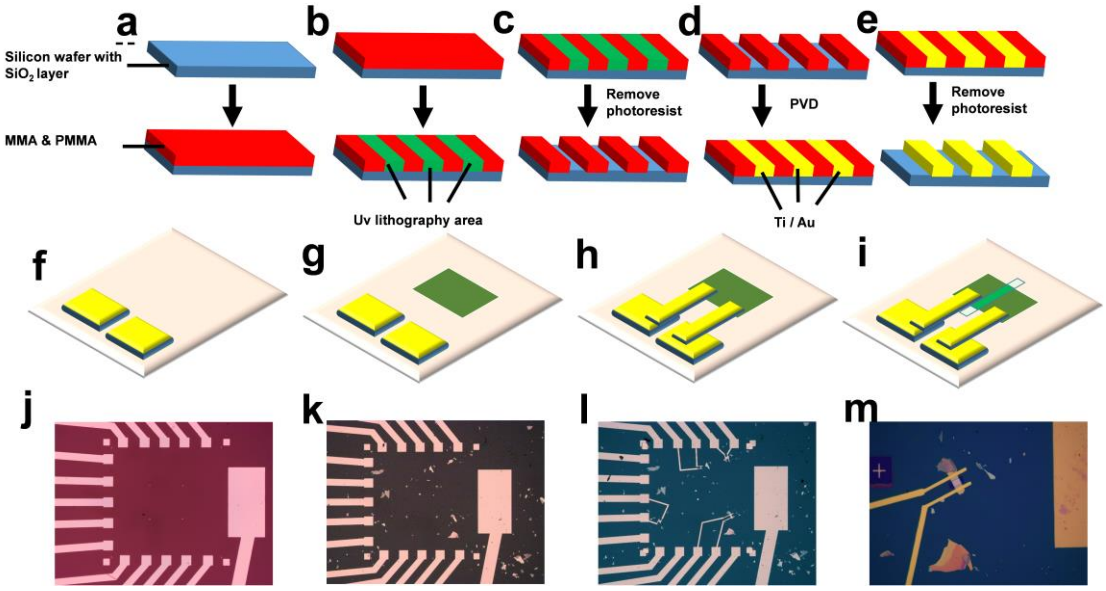

Fig S1. Fabrication process of the individual MoS_2 nanosheet based HER device. Step1, (a-e) The assembly process of outer electrodes. A suitable sized silicon wafer substrate (with a 300-nm-thick insulation layer) was cut using a silicon knife and ultrasonically cleaned with acetone. The LOR3A and S1805 photoresists were spin-coated on silicon wafers at 3000 rpm for 40 s and the prepared silicon wafers were baked at 180 ℃ for 5 minutes. Then the device was patterned by ultraviolet lithography for 1.5 s and deposited a certain thickness of Ti (5nm) and Au (25nm) by physical vapor deposition (PVD). Finally, the photoresist was washed away with acetone to obtain an outer electrode. Step 2, The assembly process of the HER device. Firstly, MoS_2 nanosheets were obtained on the outer electrode by mechanical exfoliation method, and then Methyl Methacrylate (MMA) and Poly Methyl Methacrylate (PMMA) photoresists were spin-coated on the devices at 500 rpm for 10 s and 4000 rpm for 40 s, respectively. The devices were baked at 180 ℃ for 5 minutes or 60 ℃ for 500 s. E-beam lithography (EBL) and PVD were used to obtain Ti/Au (5 nm/80 nm) inner electrodes which connect the MoS_2 nanosheets to the outer electrodes. Finally, a layer of PMMA insulating layer was spin-coated and the area to be tested is exposed by EBL. One electrode was connected to only one MoS_2 nanosheet to ensure that each MoS_2 was accurately measured. (f-i) The schematic diagram of the assembly process. (j-m) The optical image of the assembly process.

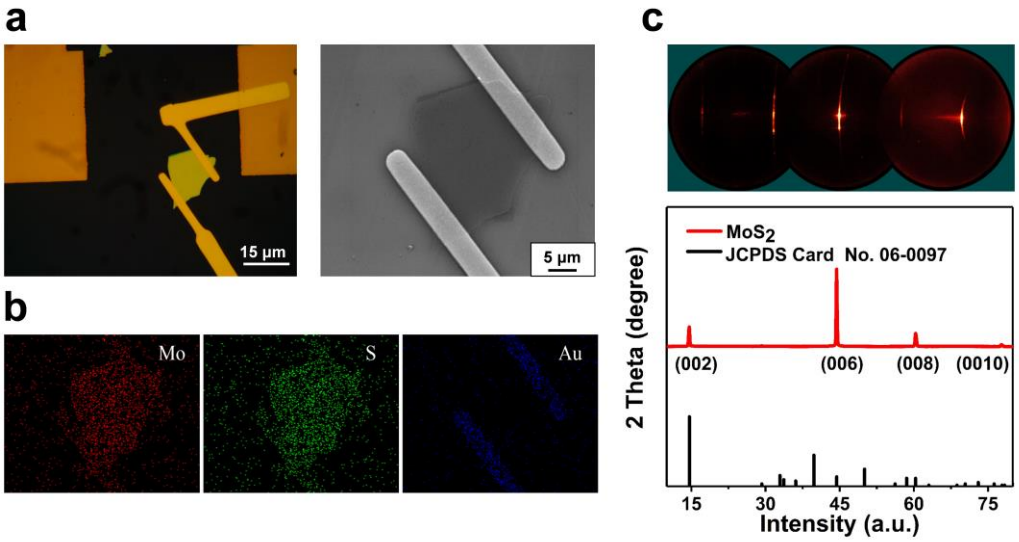

Fig S2. (a) Optical micrograph and scanning electron microscope (SEM) image of a typical MoS_2 nanosheet with two gold electrodes. (b) Corresponding elemental mapping of a typical MoS_2 nanosheet with two gold electrodes. (c) The 2D X-ray diffraction spectrum and the corresponding pattern.

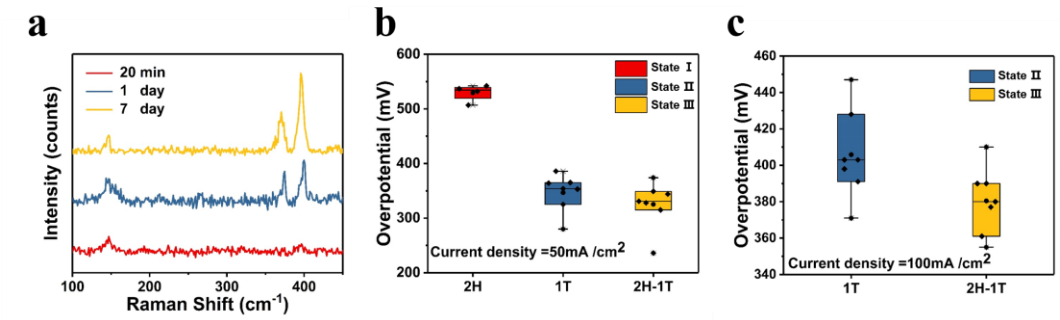

Fig S3. (a) Raman spectra of final product at different time. (b) Box plot of overpotential at current density of 50 mA/cm^2. (c) Box plot of overpotential at current density of 100 mA/cm^2. (Seven sets of data were collected.)

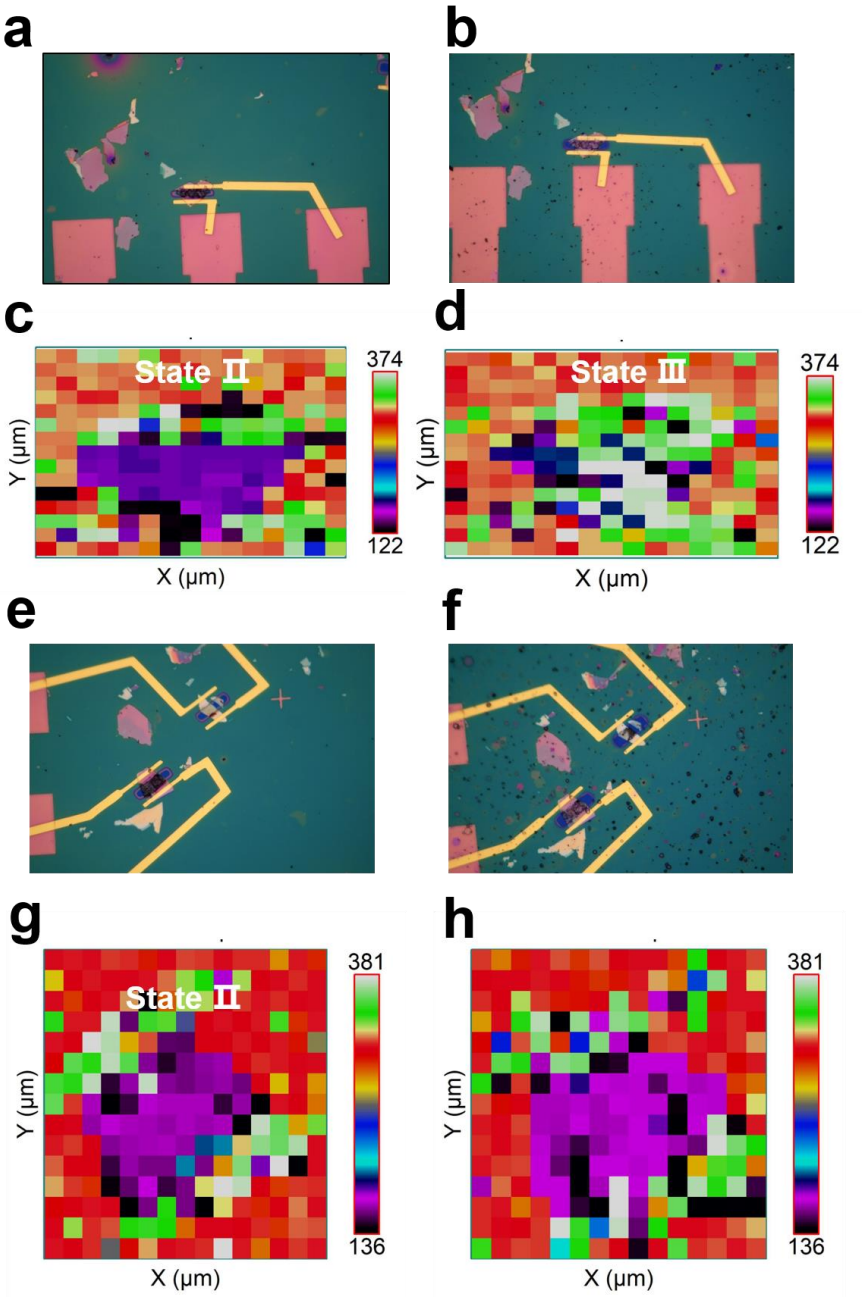

Fig S4. The in situ position Raman mapping of the 1T MoS_2. Different color intensities represent different Raman shift. The color of the point in Raman mapping represents the strongest peak of the point. For example, there are a large number of purple areas in the middle of Fig c, this means that most of the middle area corresponds to the peak in the Raman shift range from 120 cm^{-1} to 160 cm^{-1}, which includes the J_1 (156 cm^{-1}) peak. In other words, there are a large number of high intensity J_1 peaks in the middle area. And in Fig d, most of the purple areas in the middle have disappeared, which indicates that the content of the J_1 peak has decreased.

The images of (a)-(d) are the experimental group.

(a) Optical microscope image of the state Ⅱ. (b) Optical microscope image of the state Ⅲ. (c) Raman mapping corresponding to (a). (d) Raman mapping corresponding to (d).

The images of (e)-(h) are the control group, and only dip the device in H_2SO_4 for 20 minutes.

(e) Optical microscope images of the state Ⅱ. (f) Optical microscope image of the state Ⅱ after dipping. (g) Raman mapping corresponding to (e). (h) Raman mapping corresponding to (f).

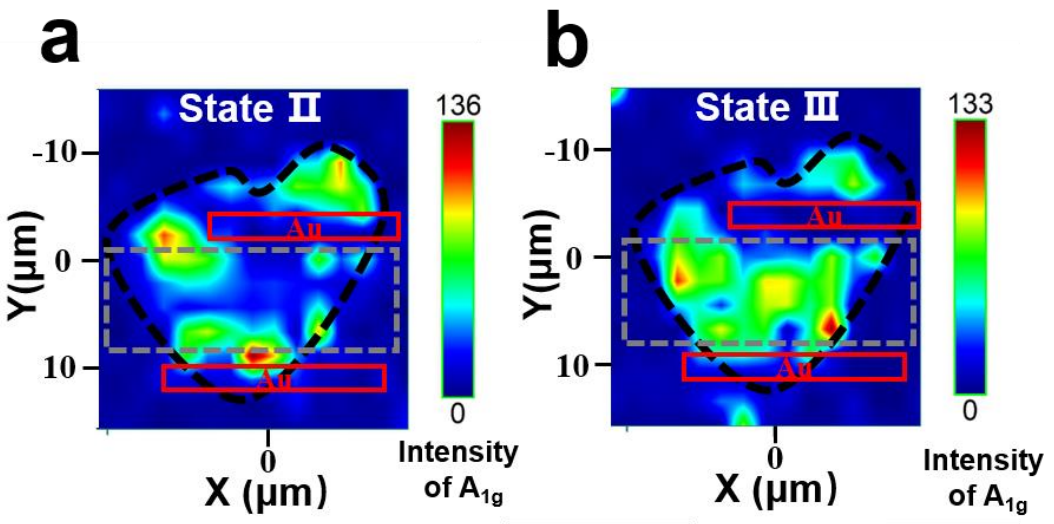

Fig S5. (a) Raman mapping of the A_{1g} peak under state II. The intensity of the A_{1g} peak is low throughout the region (b) Raman mapping of the A_{1g} peak under state III. The intensity of the A_{1g} peak is greatly increased throughout the region, but a small portion remains low.

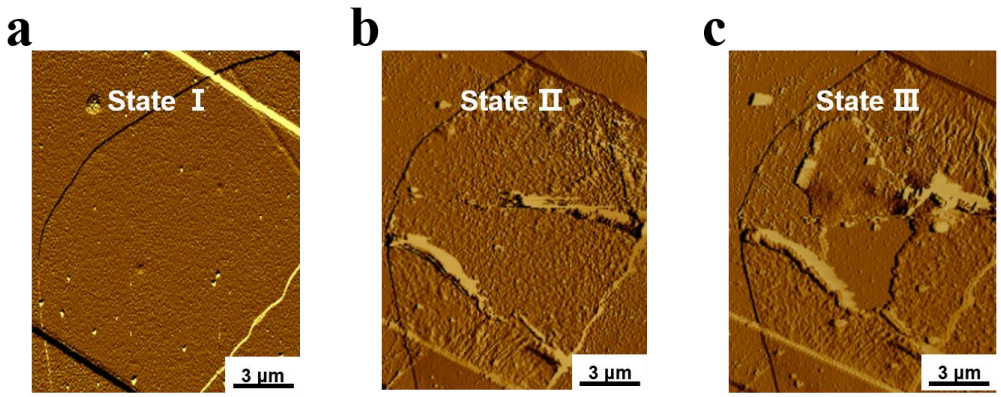

Fig S6. Topographic atomic force microscope image of MoS_2 due to excessive hydrogen evolution. (a) State I. (b) State II. (c) State III.

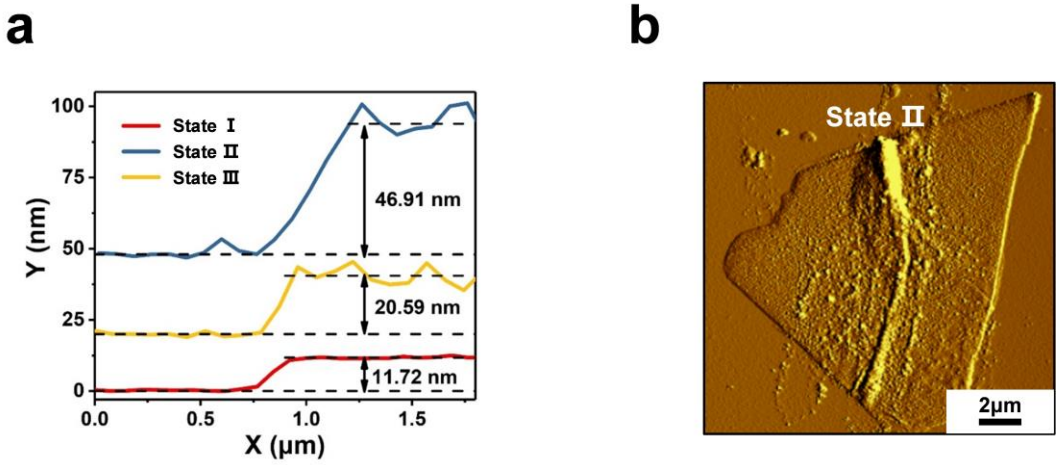

Fig S7. (a) The thickness of Fig 4d, 4e and 4f. (b) AFM image of MoS_2 after lithiation to State Ⅱ (1T phase) and there is no significant change in the surface of the sample compared to Fig 4f (The state after lithiation and annealing).

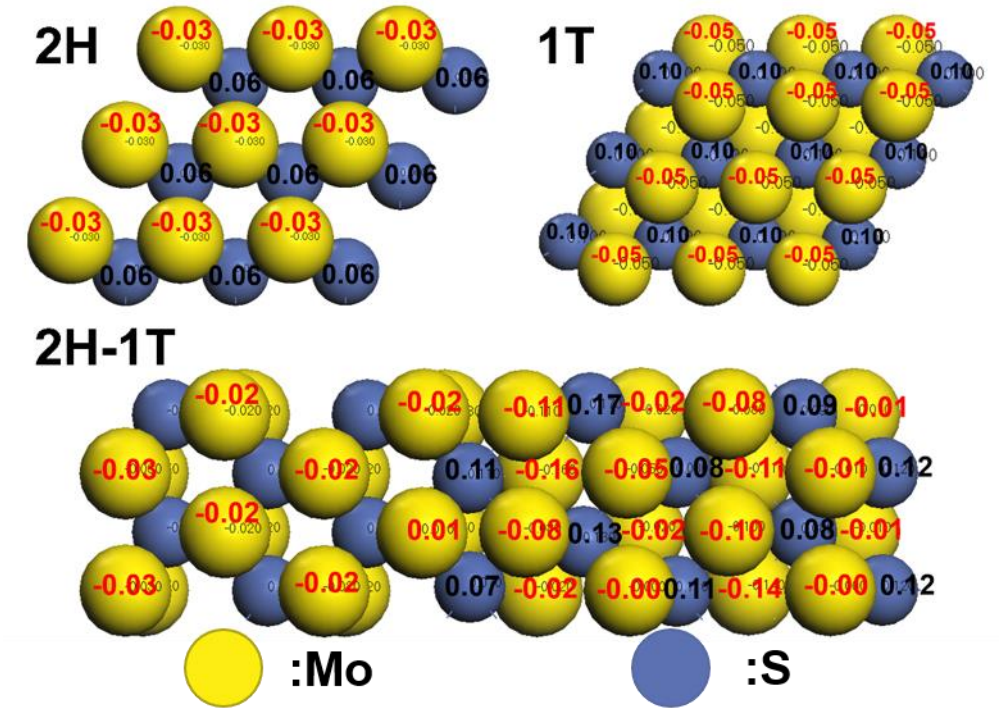

Fig S8. Structural model and the electronegativity of the three states.

Table S1. A comparison of the HER performance in this work with 2D MoS2-based electrocatalysts layed on substrates.

Catalysts	Substrates	Current density ($mA\ cm^{-2}$)	Overpotential (mV)	Tafel slope ($mV\ dec^{-1}$)	Ref
Monolayer 2H-MoS_2	Glassy Carbon	1	> 400	140-150	1
Bilayer 2H-MoS_2	Glassy Carbon	1	> 400	140-150	1
Trilayer 2H-MoS_2	Glassy Carbon	1	> 400	140-150	1
1T-MoS_2	SiO_2/ Si	10	170	100	2
2H-MoS_2	SiO_2/ Si	50	470	180	2
Monolayer 2H-MoS_2	Glassy Carbon	Onset	200	70	3
		400	450		
Monolayer 1T-MoS_2	SiO_2/ Si	10	356 ± 41	68 ± 10	4
2H-MoS_2	SiO_2/ Si	10	240	200	5
2H-1T MoS_2	**SiO_2/ Si**	**10**	**194.8**	**113.1**	**This work**

Supporting Reference

1. Yu, Y.; Huang, S. Y.; Li, Y.; Steinmann, S. N.; Yang, W.; Cao, L., *Nano Lett.* **2014,** *14*, 553-558.
2. Yu, Y.; Nam, G. H.; He, Q.; Wu, X. J.; Zhang, K.; Yang, Z.; Chen, J.; Ma, Q.; Zhao, M.; Liu, Z*., et al.*, *Nat. Chem.* **2018,** *10*, 638–643.
3. Voiry, D.; Fullon, R.; Yang, J.; de Carvalho Castro, E. S. C.; Kappera, R.; Bozkurt, I.; Kaplan, D.; Lagos, M. J.; Batson, P. E.; Gupta, G.*, et al.*, *Nat. Mater.* **2016,** *15*, 1003-1009.
4. Zhang, J.; Wu, J.; Guo, H.; Chen, W.; Yuan, J.; Martinez, U.; Gupta, G.; Mohite, A.; Ajayan, P. M.; Lou, J., *Adv. Mater.* **2017,** *29*, 1701955.
5. Wang, J.; Yan, M.; Zhao, K.; Liao, X.; Wang, P.; Pan, X.; Yang, W.; Mai, L., *Adv. Mater.* **2017,** *29*, 1604464.